Neurobiology of Disease

A TIGAR-Regulated Metabolic Pathway Is Critical for Protection of Brain Ischemia

Mei Li,[1]* Meiling Sun,[1]* Lijuan Cao,[1]* Jin-hua Gu,[1] Jianbin Ge,[2] Jieyu Chen[1], Rong Han,[1] Yuan-Yuan Qin,[1] Zhi-Peng Zhou,[3] Yuqiang Ding,[4] and Zheng-Hong Qin[1]

[1]Department of Pharmacology and Laboratory of Aging and Nervous Diseases, Jiangsu Key Laboratory of Translational Research and Therapy for Neuro-Psycho-Diseases, Soochow University School of Pharmaceutical Science; Suzhou 215123, China, [2]The Second People's Hospital of Nantong, Nantong 226002, China, [3]Department of Radiology, Affiliated Hospital of Guilin Medical College, Guilin 541001, China, and [4]Key Laboratory of Arrhythmias, Ministry of Education, East Hospital, Tongji University School of Medicine, Shanghai 200092, China

TP53-induced glycolysis and apoptosis regulator (TIGAR) inhibits glycolysis and increases the flow of pentose phosphate pathway (PPP), which generates NADPH and pentose. We hypothesized that TIGAR plays a neuroprotective role in brain ischemia as neurons do not rely on glycolysis but are vulnerable to oxidative stress. We found that TIGAR was highly expressed in brain neurons and was rapidly upregulated in response to ischemia/reperfusion insult in a TP53-independent manner. Overexpression of TIGAR in normal mice with lentivirus reduced ischemic neuronal injury, whereas lentivirus-mediated TIGAR knockdown aggravated it. In cultured primary neurons, increasing TIGAR expression reduced oxygen and glucose deprivation (OGD)/reoxygenation-induced injury, whereas decreasing its expression worsened the injury. The glucose 6-phosphate dehydrogenase was upregulated in mouse and cellular models of stroke, and its upregulation was further enhanced by overexpression of TIGAR. Supplementation of NADPH also reduced ischemia/reperfusion brain injury and alleviated TIGAR knockdown-induced aggravation of ischemic injury. In animal and cellular stroke models, ischemia/reperfusion increased mitochondrial localization of TIGAR. OGD/reoxygenation-induced elevation of ROS, reduction of GSH, dysfunction of mitochondria, and activation of caspase-3 were rescued by overexpression of TIGAR or supplementation of NADPH, while knockdown of TIGAR aggravated these changes. Together, our results show that TIGAR protects ischemic brain injury via enhancing PPP flux and preserving mitochondria function, and thus may be a valuable therapeutic target for ischemic brain injury.

Key words: **glucose 6-phosphate dehydrogenase; ischemia/reperfusion; mitochondria; NADPH; pentose phosphate pathway; TIGAR**

Introduction

Cerebral reperfusion injury aggravates ischemic brain damage mainly due to the marked increases in the generation of ROS (Crack and Taylor, 2005; Webster et al., 2006; Chen et al., 2011). During reperfusion, the mitochondria are main contributors of ROS at early stages, because of the uncoupling of oxidation and phosphorylation (Balaban et al., 2005; Lin and Beal, 2006), while NADPH oxidases (NOXs) become the main source of ROS at the later stage (Bedard and Krause, 2007; Kleinschnitz et al., 2010). NADPH is mainly produced through the pentose phosphate pathway (PPP). The NADPH is a coenzyme that is widely involved in a broad range of oxidation-reduction reactions. The NADPH is important for maintenance of the levels of reduced GSH (Bensaad et al., 2006), which is an important endogenous antioxidant mechanism. NADPH can provide energy with the isocitrate aid shuttle into the mitochondria to maintain cell energy homeostasis (Urner and Sakkas, 2005; Stanton, 2012).

TP53-induced glycolysis and apoptosis regulator (TIGAR) has a similar sequence to the bisphosphatase domain (FBPase-2) of the bifunctional enzyme 6-phosphofructo-2-kinase/fructose-2,6-bisphosphatase (PFKFB; Bensaad et al., 2006; Li and Jogl, 2009), which is a master regulator of glycolysis through its ability to synthesize fructose-2,6-bisphosphate (Fru-2,6-P_2), the most potent allosteric activator of 6-phosphofructo-1-kinase (PFK-1). Therefore, TIGAR can block glycolysis by reducing the levels of Fru-2,6-P_2 and increasing PPP (Bensaad et al., 2006; Yin et al., 2012). Glucose 6-phosphate dehydrogenase (G6PD) is a rate-limiting enzyme in PPP (Jain et al., 2004), and thus, the levels of G6PD will also determine the flux of PPP and the rate of NADPH generation. It is well known that neurons have a lower glycolytic rate than that of astrocytes (Almeida et al., 2001) and when stressed they are unable to upregulate glycolysis because of the absence of 6-phosphofructo-2-kinase/fructose-2, 6-bisphos-

Received Oct. 23, 2013; revised April 14, 2014; accepted April 18, 2014.

Author contributions: Z.-H.Q. and Y..D. designed research; M.L., M.S., L.C., J.C., and Y.-Y.Q. performed research; R.H. and Z.-P.Z. contributed unpublished reagents/analytic tools; J.-h.G. and J.G. analyzed data; Z.-H.Q., M.L., and Y.D. wrote the paper.

The Natural Science foundation of China (No. 30930035, No. 91232724, No. 81271459, and No. 81000496), "973" project from the Ministry of Science and Technology of China (2011CB51000), the Priority Academic Program Development of Jiangsu Higher Education Institutes, and the Graduate Education Innovation Project of Jiangsu Province (CXZZ12_0850).

*M.L., M.S., and L.C. contributed equally to this work.

The authors declare no competing financial interests.

Correspondence should be addressed to either of the following: Zheng-Hong Qin, PhD, Department of Pharmacology and Laboratory of Aging and Nervous Diseases, Soochow University School of Pharmaceutical Science, 199 Ren Ai Road, Suzhou 215123, China, E-mail: qinzhenhong@suda.edu.cn; or Yuqiang Ding, PhD, Key Laboratory of Arrhythmias, Ministry of Education, East Hospital, Tongji University School of Medicine, 1239 Siping Road, Shanghai 200092, China, E-mail: dingyuqiang@gmail.com.

DOI:10.1523/JNEUROSCI.4655-13.2014

 0270-6474/14/347458-14$15.00/0

phatase-3 (PFKFB3; Almeida et al., 2004). Therefore, neurons may use glucose to maintain their antioxidant status through the PPP under the condition of oxidative stress (Herrero-Mendez et al., 2009). The protection offered by this metabolic pathway may be significant as PPP provides NADPH for antioxidative stress and energy supply and pentose for DNA repair. We thus are encouraged to explore if TIGAR could be upregulated in response to ischemia/reperfusion insult and its induction could increase endogenous antioxidant capability and protect mitochondria through the PPP in neurons, thus protecting neurons against ischemic injury.

Materials and Methods

Animals and middle cerebral artery occlusion/reperfusion. Male ICR mice, 25–30 g, were purchased from SLACCAL Lab Animal. All animals were used in accordance with the institutional guidelines for animal use and care and the study protocol was approved by the ethical committee of Soochow University. Middle cerebral artery occlusion (MCAO) surgery was performed as described previously (Clark et al., 1997). Briefly, mice were anesthetized with intraperitoneal injection of 1% pentobarbital sodium. Cerebral focal ischemia was produced by intraluminal occlusion of the right MCA using a silicone-coated nylon (6-0) monofilament (Doccol). After 2 h of occlusion, filament was withdrawn to allow blood reperfusion. Cerebral blood flow was monitored (LDF ML191 Laser Doppler Blood Flow Meter) and only those mice with 90% reduction of blood flow during MCAO and 85–95% recovery of blood flow during reperfusion were used for further experiments. Sham-operated mice underwent identical surgery but the suture was not inserted. A homoeothermic heating blanket was used to maintain the core temperature at 37°C during ischemia/reperfusion operation. Mice were killed post ischemia/reperfusion at indicated time.

Assessment of infarct size. Brain infarct size was determined by staining with 1% 2,3,5-triphenyltetrazolium chloride (TTC; Sinopharm Chemical Reagent) and was analyzed with image analysis software (Image Pro Plus; Media Cybernetics). Briefly, 24 h after reperfusion, the mice were killed and brain was cut into five slices with brain-cutting matrix (ASI Instruments). Then the slices (2 mm) were bathed in the TTC solution at 37°C for 30 min. The TTC-stained brain slices were mounted on dry paper and photographed with a digital camera. The presence or absence of infarction was determined by examining TTC-stained sections for the areas on the side of infarction that did not stain with TTC. Infarct volume was expressed as a percentage of total hemisphere (Clark et al., 1997).

Assessment of neurological score and brain water content. After 24 h of post ischemia/reperfusion survival period, neurological assessment was performed using a 5-point scoring system (Longa et al., 1989). The following scale rating was used: 0, normal motor function; 1, flexion of torso and contralateral forelimb when mouse is lifted by the tail; 2, circling to the contralateral side when mouse held by the tail on a flat surface but normal posture at rest; 3, leaning to the contralateral side at rest; 4, no spontaneous motor activity. Neurological assessment was performed by an investigator blinded to the experimental treatments.

After the wet weight of the brains was quantified, the red and white parts of these brains were desiccated at 105°C for 48 h until the weight was constant. The total weight of the dried TTC-stained brains was obtained, and the water content of each brain was measured as follows: water content = (wet weight − dried weight)/wet weight × 100% (Mdzinarishvili et al., 2007).

Brain tissue mRNA isolation and real-time reverse transcription PCR. After reperfusion, brain tissues from the ischemic cortex were obtained and total RNA isolated using RNAiso Plus reagent (Takara Bio). Then, mRNA was used for the reverse transcription reaction using Prime Script RT-PCR kit (Takara Bio). The following primers were used for RT-PCR: TIGAR: forward 5′- CGCGCTTCGCCTTGACCG-3′; reverse 5′-TTGCCTTCCGCGACTCCG-3′ and β-actin: forward 5′-AAGGACTCCTATAGTGGGTGACGA-3′; reverse 5′-ATCTTCTCCATGTCGTCCCAGTTG-3′.

Lentivirus production. The mouse TIGAR cDNA was amplified with PCR, sequenced, and subcloned into a pGLV-EF1a/Lenti vector with BamH1/Pme1 restriction sites to construct a pGLV-EF1a-EGFP/Lenti-TIGAR vector (LV-TIGAR). The short hairpin RNA (shRNA)-mediated TIGAR knockdown vector was constructed by subcloning the H1 promoter-sh_TIGAR cassette into the BamH1/EcoR1 sites of the pGLV vector (LV-sh_TIGAR). The infectious lentivirus was produced by transfecting lentivector and packaging vectors into HEK293T cells. All vectors and the lentivirus of the shRNA-mediated TP53 knockdown were purchased from GenePharma.

In vivo *lentivirus and drug administration.* For lentivirus infusion, lentiviral vectors encoding TIGAR (LV-TIGAR, 1×10^9 transduction units/ml) or empty lentiviral vectors (control), lentiviral vectors encoding sh_TIGAR (LV-sh_TIGAR), or lentiviral vectors encoding sh_scramble were injected into the right lateral ventricle (0.4 mm anterior to the bregma, 0.8 mm lateral, 2.5 mm deep) and striatum (0.4 mm anterior to the bregma, 1.8 mm lateral, 3.5 mm deep; 2 μl/injection site). The efficiency of TIGAR overexpression or knockdown was evaluated with GFP fluorescence in brain sections and Western blot analysis in cortical tissues. Three weeks later, ischemia/reperfusion was performed in these animals. NADPH (2.5 mg/kg; Beyotime) was administered by intraventricular injections at the onset of the reperfusion to the normal mice or mice received LV-TIGAR or LV-sh_TIGAR. The effects of NADPH, NADPH + TIGAR overexpression, and NADPH + TIGAR knockdown on ischemic brain injury were assessed 24 h after reperfusion or long-term recovery 28 d after stroke. In other experiments, mice were given NADPH by tail vein injections (2.5 mg/kg, i.v.) before the onset of the reperfusion. The brain levels of NADPH, GSH, and ROS were measured at indicated times. To inhibit TP53 activity, the mouse was subcutaneously injected with pifithrin-α (PFT-α; 2 mg/kg; Sigma) or vehicle (DMSO) 30 min before ischemia/reperfusion (Leker et al., 2004).

Cell culture, in vitro *drug administration, and viral infection.* ICR mouse primary neuronal cells were prepared from the cerebral cortex of day 17 embryos (E17) as described previously (Yonekura et al., 2006). Glial growth was suppressed by addition of 10 μM cytosine arabinoside. Ninety-seven percent of cultured cells were neurons at 4 d. For determining TIGAR expression in primary neurons, double immunofluorescence was performed at 11 d. For detection of TIGAR expression in astrocytes, primary ICR mouse astrocytes were prepared from E17 as previously described (Tamatani et al., 2001). For manipulation of TIGAR expression, neurons were changed half of medium containing LV-TIGAR (MOI = 10) or empty lentivirus (control) and LV-sh_TIGAR or LV-sh_scramble (MOI = 10) at 4 d, and then changed back to the regular medium after 2 h. Culture was continued until 11 d. The efficiency of TIGAR overexpression or knockdown was evaluated with GFP fluorescence and Western blot analysis. To determine the role of free radicals in TIGAR-mediated effects, primary neurons (11 d) were treated with 10 μM NADPH for 4 h before oxygen glucose deprivation (OGD). Then cells were then subjected to OGD/reoxygenation for 24 h (in the presence of NADPH). For knockdown of TP53 protein, neurons were changed half of medium containing LV-sh_p53 (MOI = 20) or LV-sh_scramble (MOI = 20) at 4 d, and then changed back to the regular medium after 2 h. Culture was continued until to 11 d. To inhibit TP53, primary neurons (11 d) were treated with 30 μM PFT-α for 30 min. Cells were then subjected to OGD/reoxygenation for 3 h. DMSO only was used as vehicle control.

OGD/reoxygenation of primary neurons. The cultured primary neurons (11 d) were rinsed three times with PBS and incubated with glucose-free HBSS containing the following (in mM): 116 NaCl, 5.4 KCl, 0.8 $MgSO_4$, 1.0 NaH_2PO_4, 1.8 $CaCl_2$, and 26 $NaHCO_3$, pH 7.3, and placed in a chamber (Billups-Rothenberg MC-101), which was filled with 95% N_2 and 5% CO_2 at 37°C (OGD). Control cells were placed in HBSS containing 3 mM D-glucose and incubated under normal culture conditions for the same time period. After OGD for 4 h, cultures were replaced with the normal culture medium and cultured under normal conditions for 24 h (OGD/reoxygenation).

Isolation of mitochondria from the cells and brain tissues. After reperfusion or reoxygenation for 3 h, brain tissues from the whole ischemic cortex (including core and penumbra areas) or cultured primary neu-

rons were collected and used for purification of mitochondria with a cell mitochondria isolated kit (Beyotime) and a tissue mitochondria isolation kit (Beyotime) according to the manufacturer's instructions.

Immunoblotting. For determining the regional distribution of TIGAR in brain, various brain tissues were dissected for Western blot analysis. After reperfusion or reoxygenation, brain tissues from the whole ischemic cortex (including core and penumbra areas) or cultured primary neurons were lysed and used for immunoblotting as described previously (Zhang et al., 2007). Equal amounts (10–30 μg) of total protein extracts were separated electrophoretically on 10–12% polyacrylamide gels and blotted onto nitrocellulose membranes. The nonspecific binding was blocked by incubating membranes in PBS containing 0.05% Tween 20 (v/v) and 5% nonfat milk (v/v) for 1 h. Blots were incubated with primary antibodies as follows: rabbit anti-TIGAR (1:1000; Abcam), rabbit anti-G6PD (1:1000; Cell Signaling Technology), rabbit anti-caspase-3 (1:1000; Cell Signaling Technology), mouse anti-TP53 (1:1000; Cell Signaling Technology), rabbit anti-NOX4 (1:1000; Abcam), mouse anti-Tom 40 (1:1000; Santa Cruz Biotechnology), mouse anti-α-tubulin (1:800; Santa Cruz Biotechnology), and mouse anti-β-actin (1:5000; Sigma) at 4°C overnight. After being washed, membranes were incubated with IRDye secondary antibodies (1:10,000; Li-Cor Bioscience) for 1 h at room temperature. The images of protein–antibody interaction were captured by the Odyssey infrared imaging system (Li-Cor Bioscience). The images were analyzed for final determination of protein expression with Sigma Scan Pro 5 and normalized to the loading control β-actin.

Immunofluorescence. Immunofluorescence was performed as described previously (Tamatani et al., 2001). For detection of TIGAR expression, immunofluorescence was performed with brain sections or cultured neurons. In brief, frozen brain sections (10 μm) and cultured primary neurons (day 11) were fixed in 4% paraformaldehyde, blocked with 1% normal goat serum, and incubated with specific primary antibodies as follows: NeuN (1:200; Sigma), GFAP (1:1000; Sigma), TIGAR (1:800; Abcam), microtubule-associated protein 2 (MAP-2; 1:400; Sigma), and Tom 20 (1:500; Santa Cruz Biotechnology) for 24 h. After being rinsed three times with PBS, the brain sections or cells were incubated with FITC-conjugated anti-mouse IgG (1:400; Jackson ImmunoResearch) and Cy3-conjugated anti-rabbit IgG (1:400; Jackson ImmunoResearch) for 1 h at 37°C and rinsed three times with PBS. The nuclei were counterstained with DAPI, and slides were coverslipped. The mitochondria localization of TIGAR was determined by staining cells with 1 μM MitoTracker for 30 min at 37°C 3 h after reoxygenation. Then cells were fixed and stained with anti-TIGAR antibody to determine TIGAR location. Brain sections and cultured cells were observed under a laser confocal microscope (Olympus) with a digital camera (Olympus). Digital images were recorded and analyzed using Image Pro Plus software (Media Cybernetics) and Adobe Photoshop software.

Immunogold electron microscopic examination. A total of three adult mice were used in the electron microscopic (EM) studies according to procedures described previously (Kuwajima et al., 2004). These animals were perfusion fixed with perfusate A (consisting of 4% paraformaldehyde, 0.3% glutaraldehyde, and 0.1 M phosphate buffer). Brains were removed from the skull, postfixed in fixative B (consisting of 4% paraformaldehyde, 2.5% glutaraldehyde, and 0.1 M phosphate buffer). Sections 70 nm thick were cut with an ultramicrotome (Leica 4802A) and mounted on single-slot nickel grids. For immunohistochemical EM, mouse cortex tissue sections were blocked with bovine serum albumin for 1 h after EDTA antigen retrieval and incubated with anti-TIGAR antibody (1:200) for 24 h, followed by 10 nm gold nanoparticle-conjugated secondary antibody (1:50; G740, Sigma), and analyzed with an EM (JEM-1400).

Cell viability assay and TUNEL. Cell viability of cultured primary neurons was evaluated with a nonradioactive cell counting kit (CCK-8; Dojindo) and with a colorimetric lactate dehydrogenase (LDH) cytotoxicity assay kit (Promega) according to manufacturer's protocols. TUNEL assay was performed using a kit from Beyotimeaccording to the manufacturer's instructions.

Measurement of NADPH and GSH levels. Brain NADPH and GSH concentrations were measured 3 h after reperfusion with the EnzyChrom NADP/NADPH assay kit (BioAssay Systems) and the GSH kit (Beyotime) following manufacturer's instructions. Neuronal cells transfected with LV-GFP or LV-TIGAR or LV-sh_scramble or LV-sh_TIGAR were subjected to OGD/reoxygenation. Intracellular NADPH and GSH concentrations were measured 3 h after reoxygenation using the EnzyChrom NADP/NADPH assay kit and the GSH kit (Beyotime) following manufacturer's instructions.

Measurement of ROS and mitochondrial transmembrane potential. For assessing ROS *in vivo*, dihydroethidium (DHE, 2 mg/kg; Sigma) was injected intraperitoneally 1 h after MCAO at 2 h intervals until the end of experiment. Mice were anesthetized and killed and brain sections (10 μm) were cut with a cryostat (Leica) 1 h after the last injection of DHE. The DHE fluorescence in brain sections was observed with a fluorescence microscope. *In vitro* primary neurons transfected with LV-sh_scramble or LV-sh_TIGAR were subjected to OGD/reoxygenation. Intracellular ROS and mitochondrial membrane potential were measured 3 h after reoxygenation with incubation with 10 μM dichlorodihydrofluorescein diacetate (Beyotime) or 10 μM JC-1 (Beyotime) for 30 min at 37°C. The cells were then washed twice with ice-cooled PBS followed by suspension in the same buffer. Fluorescence intensity was measured with a laser confocal microscope and flow cytometry (FACSCalibur; Becton Dickinson) using excitation and emission wavelengths of 488 and 525 nm, respectively. Mitochondrial ROS levels were measured 3 h after reoxygenation by staining cells with 1 μM MitoTracker Green FM and 5 μM Redox-Sensor Red CC-1 (Invitrogen) for 30 min at 37°C. Cells were then washed with PBS solution and observed with a laser confocal microscope.

Behavioral tests

In all animals, a battery of behavioral tests was performed 28 d after MCAO by an investigator who was blinded to the experimental conditions.

Beam walk test. A wooden beam 130 cm long and 15 mm wide was elevated 40 cm above the floor. Each elevated rat home cage was positioned at one end of the beam. The rats were placed on the far end of the beam and trained to walk the beam toward their home cage. The test distance started at 30 cm from the near end and was 100 cm total. To quantify motor deficits, the time to cross the beam was recorded from five repetitive trials intermitted by a recovery period of 15 min after each trial. A trial ended in case of incompetence to walk on the beam and falling down for two consecutive revolutions without attempting to walk on the beam. The data are presented as the mean of six trials per animal (Chen et al., 2001; Müller et al., 2008).

Rotarod test. Mice were placed on an accelerating rotarod cylinder for a 1 min adaptation period, and the time the animals remained on the rotarod was measured (Hamm et al., 1994). The speed was slowly increased from 4 to 40 rpm within 5 min. A trial ended if the animal fell off the rungs or gripped the device and spun around for two consecutive revolutions without attempting to walk on the rungs. Motor test data were analyzed as time of mean latency to fall (in seconds, three trials) on the rotarod.

The Y-maze task. The experimental apparatus consisted of a black-painted Y-maze made of plywood. Each arm of the Y-maze was 35 cm long, 25 cm high, and 10 cm wide and was positioned at an equal angle (Yamada et al., 1999). Each mouse was placed at the end of one arm and allowed to move freely through the maze during an 8 min session. A spontaneous alternation behavior (a measure of spatial memory) was defined as the entry into all three arms on consecutive choices in overlapping triplet sets. The percentage spontaneous alternation behavior was calculated as the ratio of actual to possible alternations.

Statistical analysis

Data were presented as mean ± SEM and were evaluated with one-way ANOVA with Bonferroni's multiple-comparisons *post hoc* test for comparisons of more than two means and a two-tailed Student's *t* test if two means were compared. Differences in survival rates were assessed using the log-rank test followed by Holm–Sidak method for all pairwise multiple comparisons. A difference was considered statistically significant when $p < 0.05$.

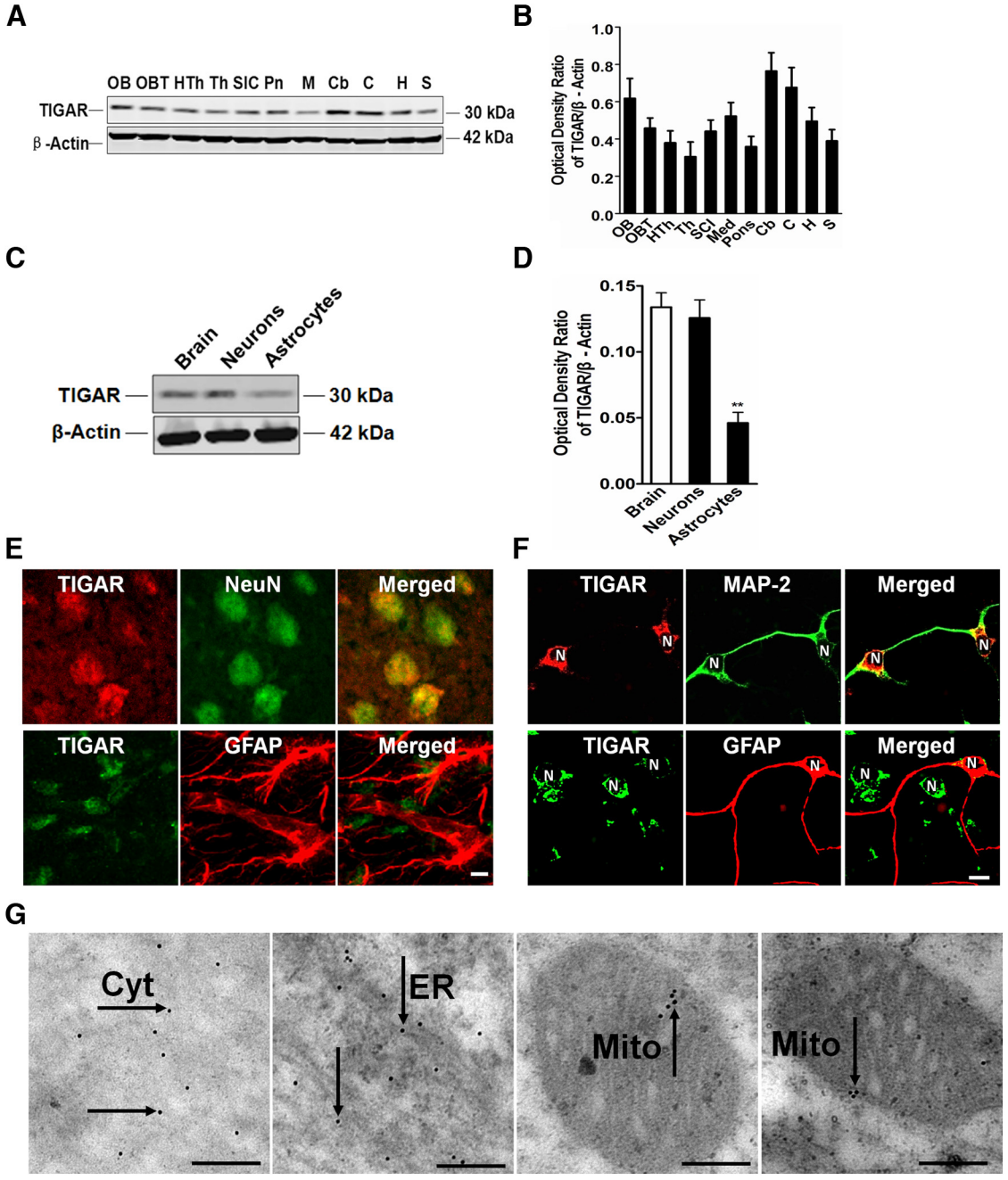

Figure 1. Regional and cellular localization of TIGAR. ***A***, ***B***, TIGAR was expressed in almost all mouse brain regions with relatively high levels in olfactory bulb, olfactory tube, and cortex. OB, olfactory bulb; OBT, olfactory bulb tube; HTh, hypothalamus; Th, thalamus; SIC, superior and inferior colliculus; Pn, pontine nuclei; M, medullae oblongate; Cb, cerebellum; C, cortex; H, hippocampus; S, striatal. $n = 5$. ***C***, ***D***, Levels of TIGAR in ICR mouse brain, cultured primary cortical neurons, and astrocytes. Data are expressed as mean ± SEM. Results were repeated in three independent experiments ($n = 5$; two-tailed t test, $^{**}p < 0.01$ vs neurons). ***E***, Immunofluorescence of TIGAR in mouse brain. Double immunofluorescence of TIGAR and with GFAP (astrocytes marker) or NeuN (neuronal marker) was performed. TIGAR was predominantly expressed in cortical neurons. Scale bar, 10 μm. ***F***, Representative immunofluorescence image of TIGAR in mixed culture of primary neurons and astrocytes. Double immunofluorescence of TIGAR and MAP-2 (neuronal marker) or GFAP was performed. N, nucleus. TIGAR was mainly expressed in primary neurons. Some astrocytes were weakly stained with TIGAR antibody. Scale bar, 30 μm. ***G***, Subcellular localization of TIGAR. Brain cortical tissues were stained with immunogold and examined with EM. Microphotographs showed immunoreactive elements (colloidal gold particles) in the cytoplasm (Cyt), endoplasmic reticulum (ER), and mitochondria (Mito; indicated by arrows). Scale bar, 200 nm.

Results

TP53-independent upregulation of TIGAR in response to brain ischemia/reperfusion injury

The expression and distribution of TIGAR in brain has not been characterized before. TIGAR was widely expressed in brain regions with relatively high levels in the olfactory bulb, cerebellum, and cortex (Fig. 1*A*,*B*). To learn the cellular localization of TIGAR in brain, we examined the expression of TIGAR in mouse brains and cultured neural cells. TIGAR was mainly expressed in neurons as revealed by Western blot analysis (Fig. 1*C*,*D*). Double immunostaining of brain tissues showed that most TIGAR-positive cells were NeuN-positive neurons, while much fewer TIGAR-positive cells were GFAP-positive astrocytes (Fig. 1*E*). To further confirm enrichment of TIGAR in neurons, TIGAR ex-

pression was examined in cultured primary neurons and astrocytes. In mixed culture of neurons and astrocytes, high levels of TIGAR were found in MAP-2-positive cells (neuronal marker), while low levels were detected in GFAP-positive cells (Fig. 1*F*). EM examination showed that TIGAR immunoreactivity was localized in the cytoplasm, the mitochondrial membranes, mitochondrial matrix. and endoplasmic reticulum (Fig. 1*G*).

To investigate if TIGAR was induced by ischemic insult, we examined TIGAR expression in mouse brains and cultured primary neurons after ischemia/reperfusion and OGD/reoxygenation, respectively. The results showed that ischemia/reperfusion and OGD/reoxygenation elevated TIGAR protein levels in ischemic cortex (Fig. 2*A*) and in cultured primary neurons (Fig. 2*B*). In ischemic cortex, TIGAR protein reached the peak level at 3 h post reperfusion and started to decline toward basal levels thereafter. Meanwhile, the mRNA levels of TIGAR were also markedly increased in ischemic cortex (Fig. 2*C*). As TIGAR was reported as a TP53-responsive gene, we next examined if TIGAR induction is TP53 dependent. The results showed that TP53 was upregulated in ischemic cortex (Fig. 2*D*) or primary neurons (Fig. 2*E*) that underwent ischemia/reperfusion or OGD/reoxygenation, respectively, but the time course of TP53 induction was delayed relative to TIGAR induction. Moreover, when mice were pretreated with the TP53-specific inhibitor PFT-α before ischemia/reperfusion, TIGAR upregulation was not significantly affected (Fig. 2*F*), while the same dose of PFT-α did block the upregulation of TP53 target gene Bax after reperfusion (Fig. 2*G*). Similar results were obtained in OGD/reoxygenation neurons (Fig. 2*H*,*I*). Furthermore, knockdown of TP53 with LV-sh_TP53 in cultured primary neurons inhibited OGD/reoxygenation-induced Bax induction but had no effect on TIGAR expression (Fig. 2*J*,*K*).Together, these results indicated that TIGAR was rapidly upregulated in response to ischemia/reperfusion injury, largely in a TP53-independent fashion.

Critical role of TIGAR in ischemia/reperfusion injury

To explore the role of TIGAR in cerebral ischemic injury, we injected LV-TIGAR or LV-sh_TIGAR into mouse lateral ventricle and striatum. The efficiency of viral infection in mouse brain was determined by fluorescence of LV-TIGAR-GFP (Fig. 3*A*) and Western blot analysis of TIGAR protein (Fig. 3*B*). The levels of TIGAR were markedly elevated in mouse brain injected with LV-TIGAR, while significantly reduced with LV-sh_TIGAR (Fig. 3*C*). In LV-TIGAR-treated mice, overexpression of TIGAR significantly reduced the infarct size (Fig. 3*D*,*E*), neurological deficits (Fig. 3*F*), and brain edema (Fig. 3*G*). In contrast, knockdown of TIGAR with LV-sh_TIGAR markedly increased the infarct size (Fig. 3*D*,*E*), neurological deficits (Fig. 3*F*), and brain edema (Fig. 3*G*). Furthermore, overexpression of TIGAR (LV-TIGAR-treated mice) improved long-term survival and recovery of motor and cognitive functions 28 d post ischemia/reperfusion (Fig. 3*H*). In contrast, knockdown of TIGAR (LV-sh_TIGAR-treated mice) suppressed the long-term survival and recovery of neurological functions (Fig. 3*I*–*K*). These *in vivo* results indicate the essential role of TIGAR in ischemia/reperfusion-induced brain injury.

To further explore the role of TIGAR in neuronal ischemic injury, we infected LV-TIGAR or LV-sh_TIGAR into cultured mouse primary neurons. The efficiency of viral infection in mouse primary neurons was determined by fluorescence of LV-TIGAR-GFP (Fig. 4*A*) and Western blot analysis of TIGAR protein (Fig. 4*B*). The levels of TIGAR were significantly increased in mouse primary neurons infected with LV-TIGAR, whereas it was significantly reduced in mouse primary neurons infected with LV-sh_TIGAR (Fig. 4*C*). In cultured primary neurons, overexpression of TIGAR with LV-TIGAR significantly increased cell viability and reduced LDH release under OGD/reoxygenation condition, whereas knockdown of TIGAR with LV-sh_TIGAR markedly decreased cell viability and aggravated LDH release (Fig. 4*D*,*E*). The decrease or increase in OGD/reoxygenation-induced apoptosis by overexpression or knockdown of TIGAR was also observed using TUNEL analysis (Fig. 4*F*). These results suggest that TIGAR is a critical modulator in OGD/reoxygenation-induced neuronal death.

TIGAR enhances the flux of PPP

The increase in PPP flow by TIGAR may require coordination of G6PD to provide more substrates. As expected, an increase in G6PD in ischemic cortex was observed 3–12 h after reperfusion (Fig. 5*A*,*B*). In contrast, the increase in NOX4, an enzyme that produces ex-mitochondria ROS, was not detected until 12 and 24 h after reperfusion (data not shown). The marked increases in ROS production in the ischemic cortex were seen at the onset of reperfusion (peaked 0.5 h post reperfusion) and gradually declined thereafter. A second peak of ROS production was observed 12 h after reperfusion (Fig. 5*C*,*D*), the time when TIGAR and G6PD expression had dropped to the basal levels and an induction of NOX4 was seen. Furthermore, lentivirus-mediated overexpression of TIGAR further enhanced G6PD upregulation (Fig. 5*E*,*F*), while lentivirus-mediated knockdown of TIGAR inhibited its upregulation in the ischemic cortex (Fig. 5*G*,*H*). Meanwhile, the decreases in the levels of NADPH (Fig. 5*I*) and GSH (Fig. 5*J*) in ischemic cortex was reversed by TIGAR overexpression, whereas it was exacerbated by TIGAR knockdown.

In vitro, OGD/reoxygenation also induced the upregulation of G6PD levels in primary neurons (Fig. 6*A*,*B*), and the effect was further strengthened by the overexpression of TIGAR (Fig. 6*C*,*D*), but was tempered by the knockdown of TIGAR (Fig. 6*E*,*F*). Consistently, TIGAR overexpression elevated, whereas TIGAR knockdown decreased NADPH and GSH levels in cultured primary neurons under OGD/reoxygenation condition (Fig. 6*G*,*H*). Finally, we evaluated if OGD/reoxygenation-induced increases in intracellular ROS levels could be prevented by addition of exogenous NADPH. The results showed that TIGAR knockdown-induced increases in ROS were inhibited by the addition of exogenous NADPH, while TIGAR overexpression-induced decreases in ROS were further enhanced (Fig. 6*I*).Together, these results show that overexpression of TIGAR and supplementing its downstream molecules reduced ROS levels. Thus the significance of TIGAR upregulation along with G6PD might help to boost PPP to produce more NADPH, and thus to reduce ROS.

To evaluate if the neuroprotective effects by TIGAR overexpression in ischemia/reperfusion are mediated by its PPP metabolic product, we investigated the effect of exogenous NADPH on ischemia/reperfusion injury. Intraventricular injection of NADPH at the onset of reperfusion significantly reduced cerebral infarct size (Fig. 7*A*,*B*), neurological deficits (Fig. 7*C*), and brain edema (Fig. 7*D*). Moreover, supplementing NADPH significantly improved long-term survival (Fig. 7*E*) and recovery of neurological functions after ischemia/reperfusion (Fig. 7*F*–*H*). The results also demonstrated that exogenous NADPH blocked TIGAR knockdown-induced increases in brain injury, and potentiated TIGAR overexpression-induced neuroprotection against brain injury (Fig. 7*A*–*H*).

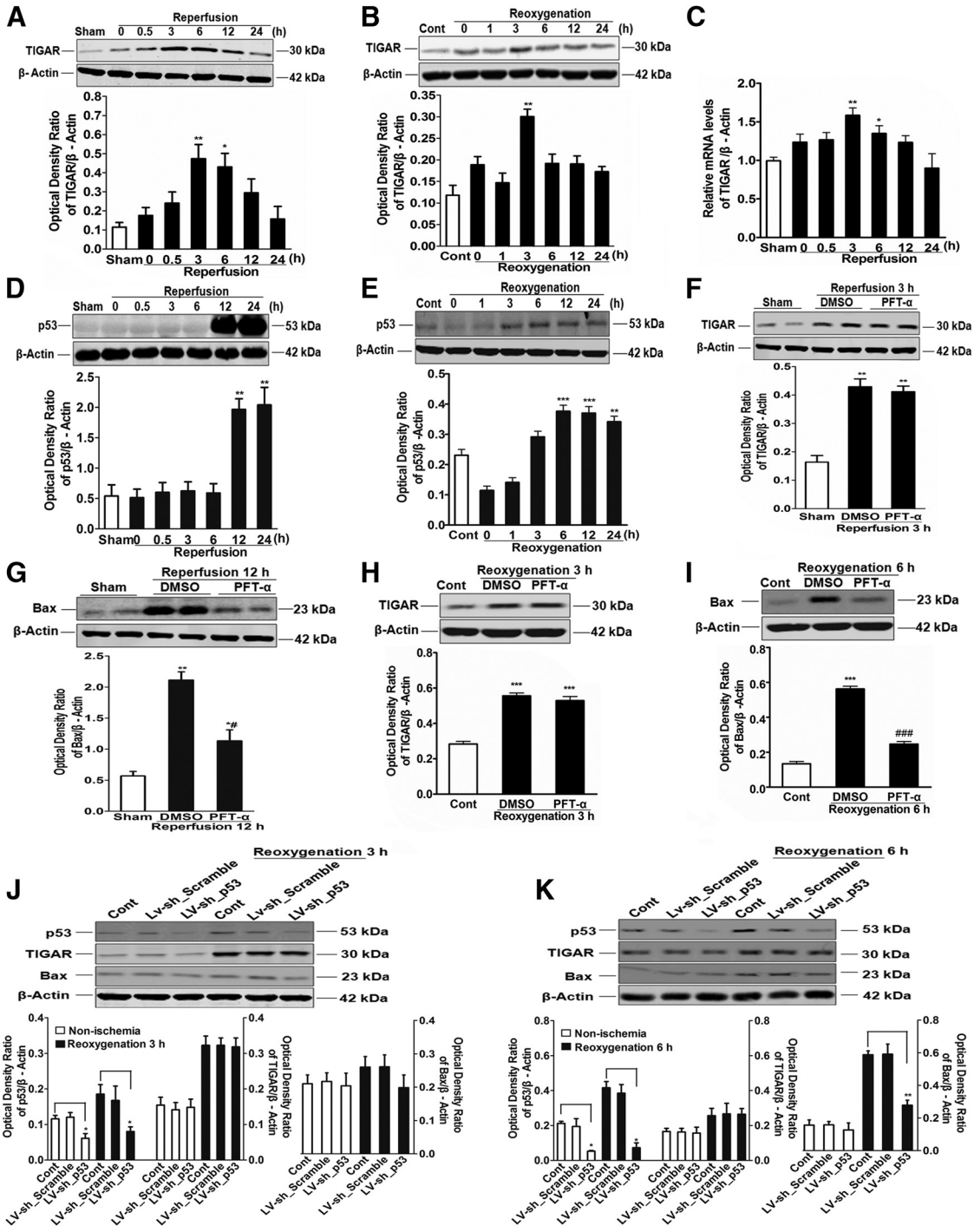

Figure 2. TIGAR upregulation in animal and cellular models of ischemia/reperfusion. ***A***, TIGAR was upregulated in the ischemic cortex after reperfusion. ***B***, TIGAR was upregulated in cultured neurons after reoxygenation. ***C***, The mRNA levels of TIGAR were increased in ischemic brain after reperfusion. ***D***, TP53 was upregulated in ischemic cortex after reperfusion. ***E***, TP53 was upregulated in cultured primary neurons after reoxygenation. ***F***, The TP53 inhibitor PFT-α showed no effect on TIGAR expression 3 h after reperfusion. ***G***, The TP53 inhibitor PFT-α significantly blocked Bax protein expression 12 h after reperfusion. ***H***, PFT-α had no effect on TIGAR expression 3 h after reoxygenation. ***I***, The TP53 inhibitor PFT-α significantly inhibited Bax protein expression 6 h after reoxygenation as compared with DMSO-treated group. ***J***, Knockdown of TP53 protein did not inhibit TIGAR expression 3 h after reoxygenation ($^{*}p < 0.05$). ***K***, TP53 knockdown significantly inhibited Bax protein expression 6 h after reoxygenation as compared with model control (Cont) group($^{**}p < 0.01$). Data are expressed as mean ± SEM. One-way analysis of ANOVA with Bonferroni's *post hoc* test, $^{*}p < 0.05$, $^{**}p < 0.01$, $^{***}p < 0.001$ versus sham or control; $^{\#}p < 0.05$, $^{\#\#\#}p < 0.001$ versus DMSO; $n = 5$.

TIGAR and NADPH preserves mitochondria membrane potential and inhibits activation of caspase-3

To further explore TIGAR's neuroprotective mechanisms, we examined mitochondrial localization of TIGAR *in vitro* after OGD/reoxygenation treatment. We found that TIGAR distribution in the mitochondria was increased in cultured primary neurons that underwent OGD/reoxygenation (Fig. 8*A*). The increase in mitochondrial localization of TIGAR in mouse cortex after 3 h of reperfusion was examined with EM. The immunogold labeling revealed an increase in mitochondrial TIGAR after ischemia/reperfusion (Fig. 8*B*). Furthermore, the increase in mitochondrial TIGAR protein was determined

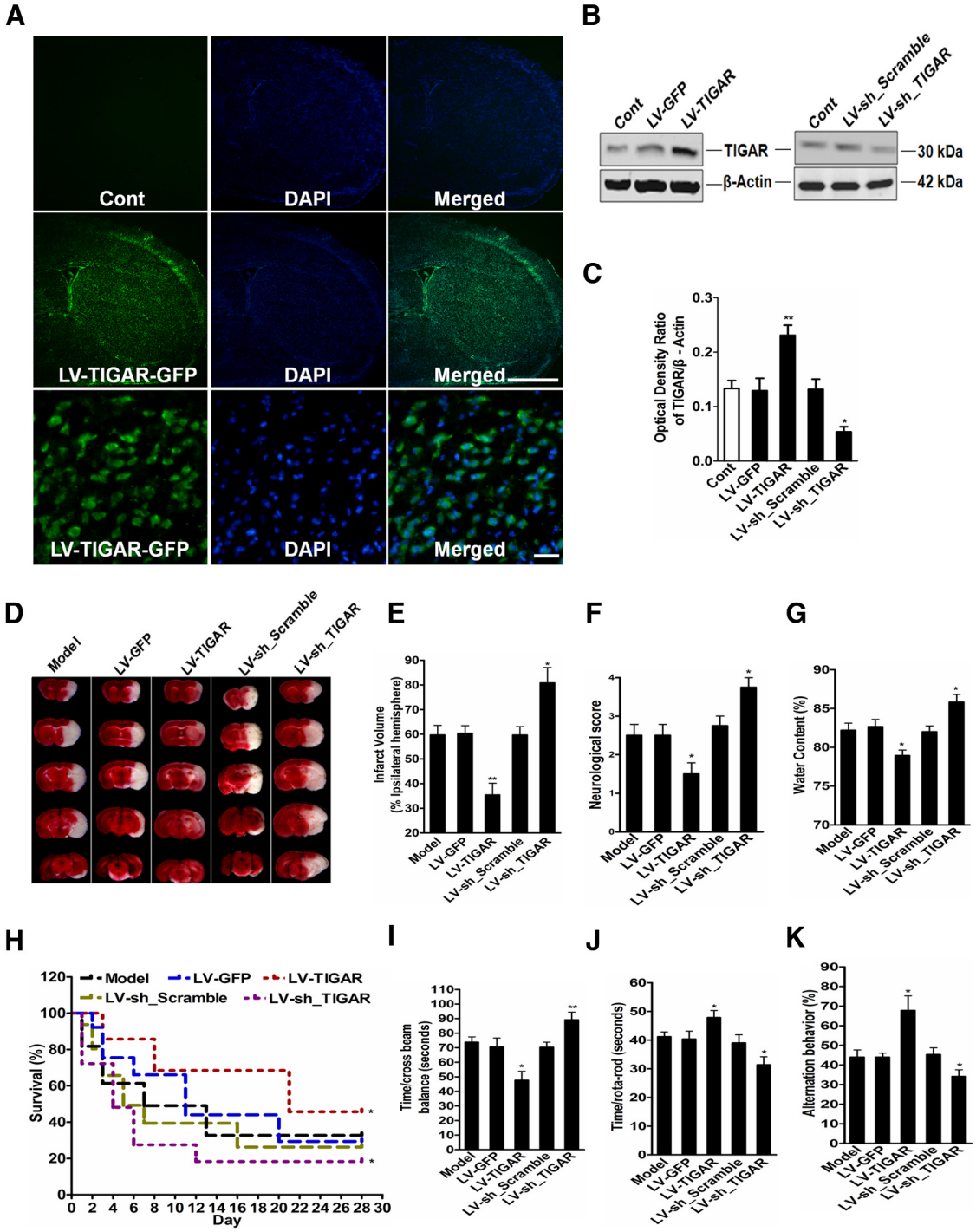

Figure 3. Alteration of levels of TIGAR affects ischemia/reperfusion injury *in vivo*. LV-TIGAR or LV-sh_TIGAR was injected into the right lateral ventricle and striatum of male ICR mouse (3 weeks, 8–9 g). Mice were subjected to MCAO/reperfusion injury 3 weeks after viral infection. ***A***, A GFP-containing lentivirus vector (LV-GFP) efficiently infected brain ($n = 5$). Scale bars: top and middle panels (in middle), 100 μm; bottom panels, 40 μm. ***B***, ***C***, Representative immunoblots and quantification showing efficiency of overexpression and knockdown of TIGAR in the cortex of mice, respectively ($n = 5$). Representative TTC staining (***D***) and quantification (***E***) of infarct size ($n = 10$). Overexpression of TIGAR by LV-TIGAR significantly reduced (***D***, ***E***), while knockdown of TIGAR by LV-sh_TIGAR increased ischemic infarct size, neurological score (***F***), and brain water content (***G***) 24 h after reperfusion. ***H***, Poststroke survival rate 28 d after stroke analyzed using log-rank test; $^{*}p < 0.05$ versus model. ***I***, Beam balance test. ***J***, Rotarod test. ***K***, Y-maze test (alternation behavior). Data were expressed as mean ± SEM. One-way ANOVA with Bonferroni's *post hoc* test, $^{*}p < 0.05$, $^{**}p < 0.01$ versus LV-GFP, $^{*}p < 0.05$ versus LV-sh Scramble; $n = 10$. Cont, control.

with immunoblotting. The results demonstrated that TIGAR protein in the mitochondrial fraction was significantly increased in primary neurons by OGD/reoxygenation (Fig. 8*C*) or in mouse cortex by ischemia/reperfusion insults (Fig. 8*D*). Oxidative stress causes the collapse of the mitochondrial transmembrane potential and activation of caspases (Niizuma et al., 2009). We demonstrated that overexpression of TIGAR prevented OGD/reoxygenation-induced decreases in mitochondrial transmembrane potential, and this effect was potentiated by the addition of NADPH. In contrast, knockdown of TIGAR exacerbated the decrement in mitochondrial transmembrane potential, but it was blocked by the addition of

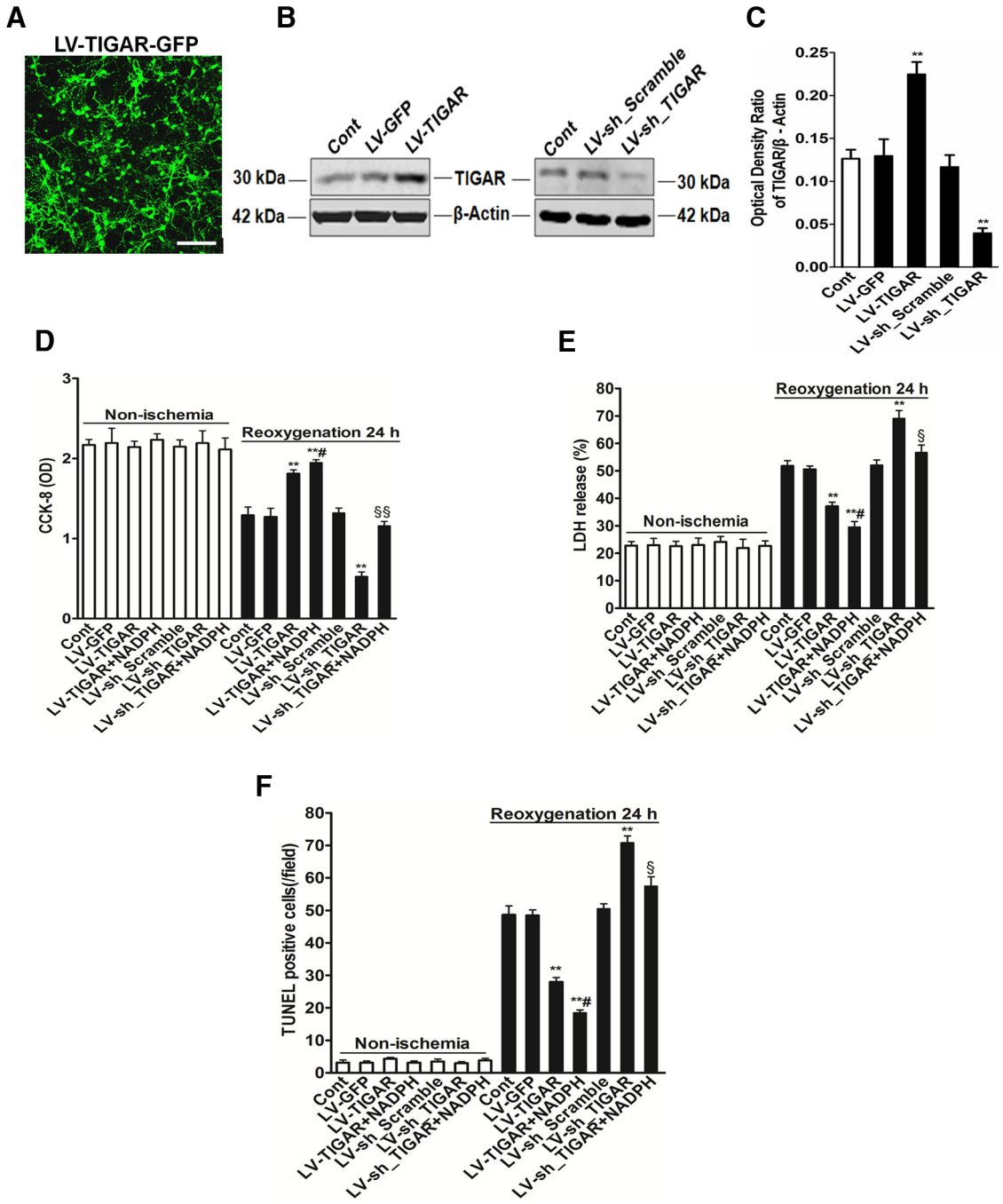

Figure 4. TIGAR reduces OGD/reoxygenation-induced neuronal death *in vitro*. Primary neurons were infected with LV-TIGAR or LV-sh_TIGAR and were treated with OGD/reoxygenation. ***A***, Cultured neurons infected with GFP-containing lentivirus (MOI = 10). Scale bar, 40 μm. ***B***, ***C***, Immunoblots and quantitative analysis of efficiency of overexpression and knockdown of TIGAR in cultured neurons infected with lentivirus. ***D–F***, Cultured primary neurons were infected with LV-TIGAR or LV-sh_TIGAR, followed by OGD/reoxygenation treatment. Primary neurons (11 d) were treated with 10 μM NADPH started 4 h before OGD/reoxygenation and continued during OGD/reoxygenation. ***D***, Cell viability was assayed with CCK-8 kit, and cell death was determined by LDH release (***E***) and TUNEL (***F***; $^{**}p < 0.01$ vs cont, $^{\#}p < 0.05$ vs LV-TIGAR, $^{\S}p < 0.05$, $^{\S\S}p < 0.01$ vs LV-sh_TIGAR under reoxygenation condition; $n = 5$). Data are expressed as mean ± SEM. One-way analysis of ANOVA with Bonferroni's *post hoc* test. Cont, control.

NADPH (Fig. 8*E*,*F*). Furthermore, overexpression of TIGAR robustly inhibited mitochondrial ROS bursting, which was enhanced by the addition of NADPH. On the other hand, knockdown of TIGAR induced increases in mitochondrial ROS bursting, which was blocked by the addition of NADPH (Fig. 8*G*). Thus, TIGAR upregulation protects mitochondrial functions under OGD/reoxygenation condition.

Apoptosis plays an important role in ischemia/reperfusion-induced neuronal death, and caspase-3 is the major executioner caspase involved in mitochondria-mediated apoptosis (Sims and Muyderman, 2010). We showed that TIGAR overexpression significantly inhibited OGD/reoxygenation-induced caspase-3 activation (Fig. 8*H*,*I*), but TIGAR knockdown aggravated it (Fig. 8*J*,*K*). Furthermore, OGD/reoxygenation-induced caspase-3 activation was decreased by the addition of NADPH (Fig. 8*L*,*M*). TIGAR knockdown significantly increased neuronal death as evidenced by the decreases in cell viability, the increases in LDH release, and more TUNEL-positive cells. All these detrimental

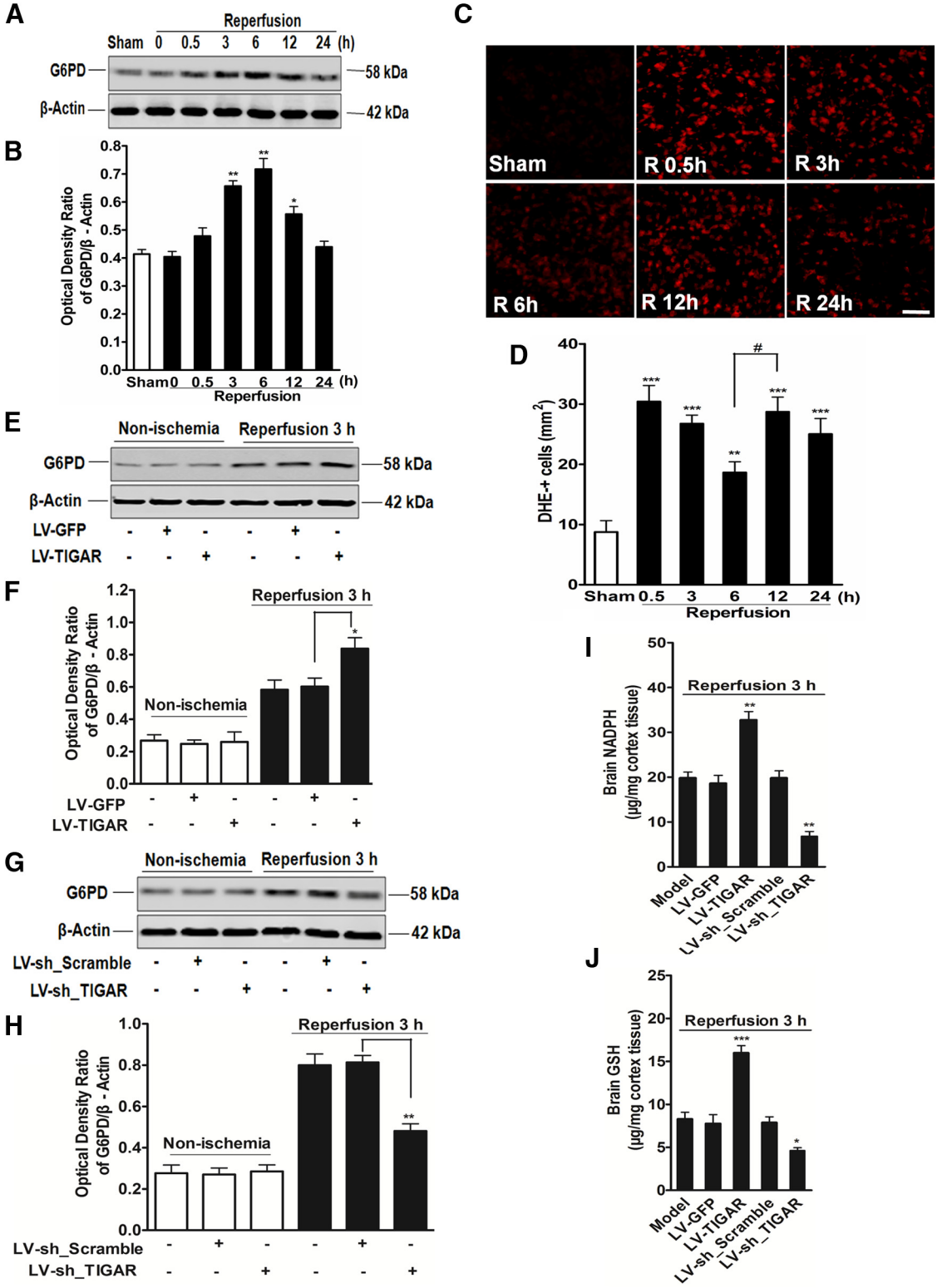

Figure 5. TIGAR increases PPP flow by regulating G6PD. ***A***, ***B***, Time course of G6PD expression after reperfusion. G6PD was upregulated in ischemic cortex 3–12 h after reperfusion ($^{*}p < 0.05$, $^{**}p < 0.01$ vs sham, $n = 5$). ***C***, ***D***, Representative photographs of DHE fluorescence analysis of the levels of ROS in ischemic cortex at indicated time points after reperfusion ($^{**}p < 0.01$, $^{***}p < 0.001$ vs sham, $^{\#}p < 0.05$, $n = 5$). Scale bar, 50 μm. Male ICR mice were infected with LV-TIGAR or LV-sh_TIGAR and were subjected to MCAO/reperfusion 3 weeks later and killed 3 h after reperfusion. ***E***, ***F***, Lentivirus-mediated TIGAR overexpression enhanced G6PD upregulation ($^{*}p < 0.05$, $n = 5$), while knockdown of TIGAR (***G***, ***H***) decreased G6PD upregulation ($^{**}p < 0.01$, $n = 5$). TIGAR overexpression increased NADPH (***I***) and GSH (***J***) levels, while TIGAR knockdown decreased them in mouse ischemic cortex ($^{**}p < 0.01$, $^{***}p < 0.001$ vs LV-GFP, $^{*}p < 0.05$, $^{**}p < 0.01$ vs LV-sh Scramble; $n = 5$). Data were expressed as mean ± SEM. One-way ANOVA with Bonferroni's *post hoc* test.

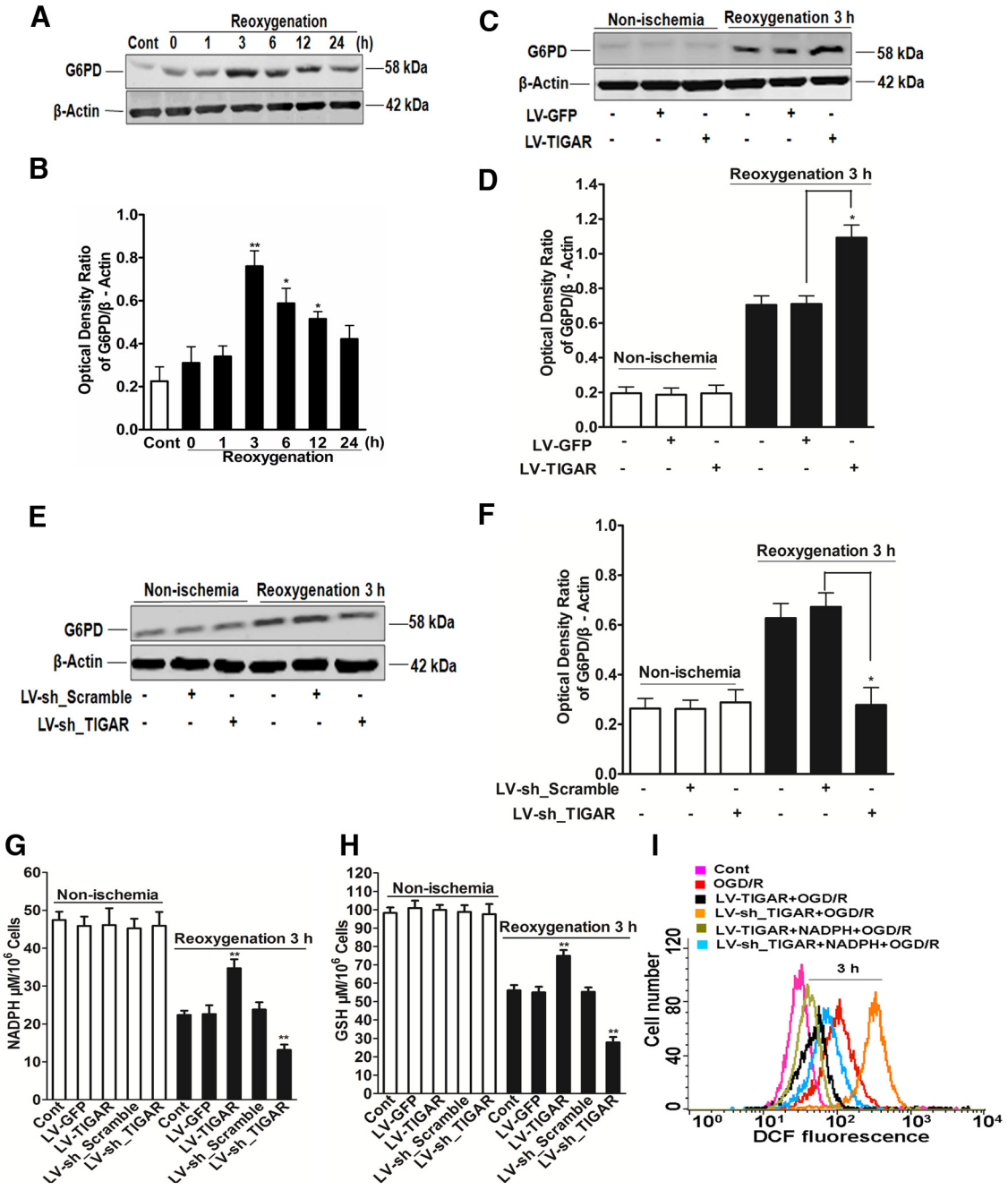

Figure 6. TIGAR reduces ROS through generating NADPH. Primary cultured neurons (4 d) were infected with LV-TIGAR or LV-sh_TIGAR and were subjected to OGD/reoxygenation 7 d later and were collected at 3 h after reoxygenation. ***A***, ***B***, G6PD was upregulated in cultured neurons 3 h after reoxygenation (*$p < 0.05$, **$p < 0.01$ vs sham, $n = 5$). Cont, control. ***C***, ***D***, Lentivirus-mediated TIGAR overexpression enhanced G6PD induction (*$p < 0.05$, $n = 5$). ***E***, ***F***, Knockdown of TIGAR decreased G6PD induction (*$p < 0.05$, $n = 5$). Neurons infected with LV-TIGAR or LV-sh_TIGAR were cultured for 11 d and treated with 10 μM NADPH 4 h before OGD/reoxygenation. The levels of NADPH (***G***) and GSH (***H***) and ROS production (***I***) were analyzed using proper assay kits and flow cytometry 3 h after reoxygenation (**$p < 0.01$ vs cont under reoxygenation condition. $n = 5$). Data were expressed as mean ± SEM. One-way ANOVA with Bonferroni's *post hoc* test.

effects were prevented by the supplementation of NADPH. Exogenous NADPH also further enhanced the beneficial effects of TIGAR overexpression on neurons under OGD/reoxygenation condition (data not shown). These data suggest that much of the neuronal protective effect of upregulation of TIGAR pathway, if not all, is achieved by inhibition of mitochondrial apoptotic pathway triggered by ROS and other signaling pathways.

Discussion

In the present study, we examined the role of TIGAR in ischemia/reperfusion-induced brain injury. We found that there was a rapid upregulation of TIGAR in response to ischemia/reperfusion insult, and TIGAR expression was positively and negatively correlated to the elevation of NADPH and ROS in ischemic brain, respectively. Manipulation of TIGAR levels significantly altered the sensitivity of neurons to ischemia/reperfusion damage and long-term postischemia survival and functional recovery. TIGAR expression increased PPP flux as evidenced by G6PD upregulation accompanied by increased NADPH, increased GSH, and decreased ROS under ischemic condition. In culture neurons and mouse cortex, OGD/reoxy-

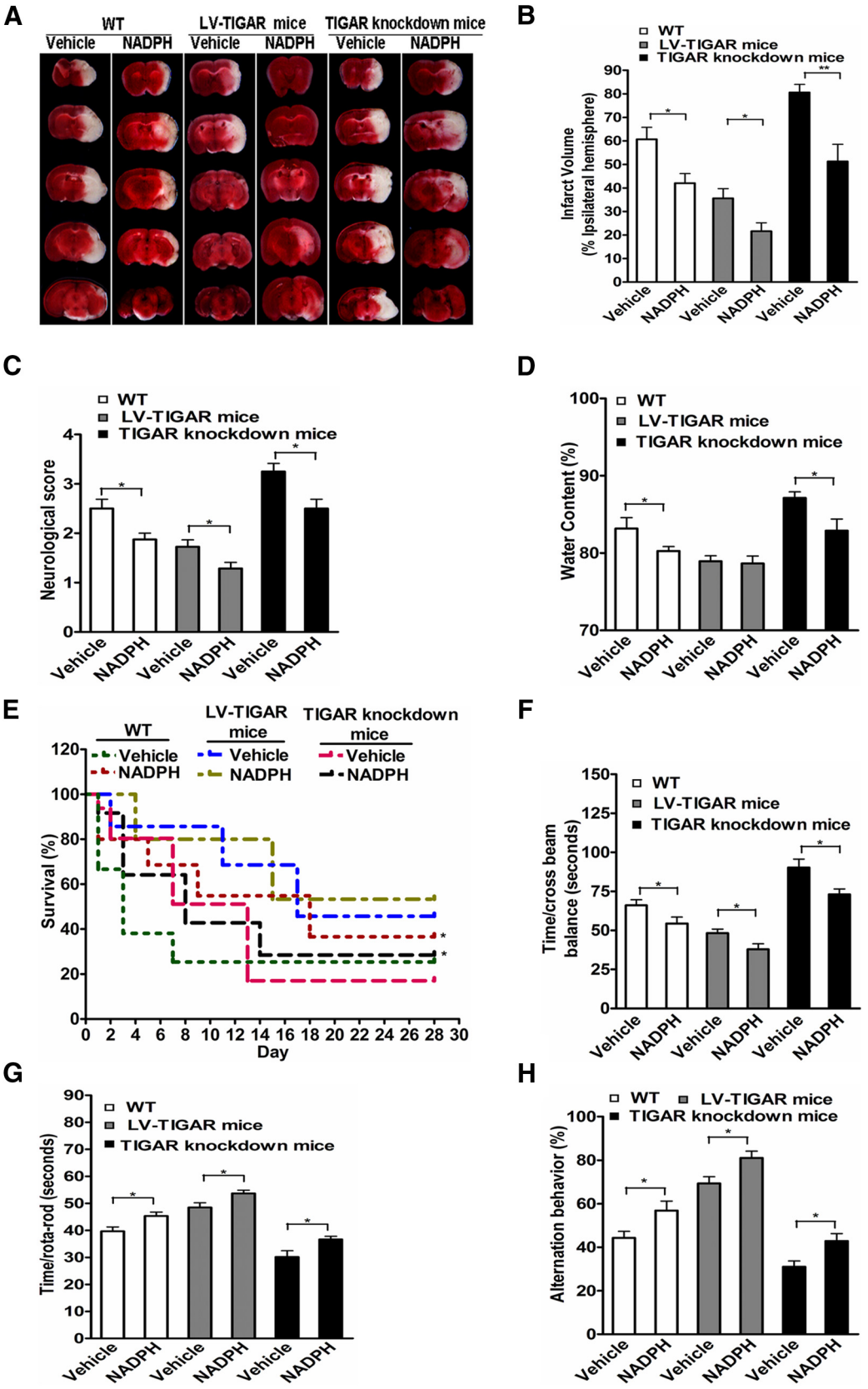

Figure 7. TIGAR protects against ischemia/reperfusion injury by increasing NADPH. ***A–D***, Applying exogenous NADPH ameliorated brain ischemia/reperfusion injury. Mice infected with lentivirus were injected with NADPH (i.c.v., 2.5 mg/kg) at the onset of reperfusion; (***A***, ***B***) infarct size, neurological score (***C***), and brain water content (***D***) were determined after 24 h reperfusion. NADPH can significantly reduce infarct size (***A***, ***B***), relieve the neurological symptoms (***C***), and reduce brain water content (***D***) in both LV-mediated TIGAR overexpression and knockdown mice 24 h after MCAO/reperfusion injury ($n = 11$). NADPH also elevated mice survival rate 28 d after stroke (***E***) and improved motor and cognitive function: beam balance test (***F***), rotarod test (***G***), and Y-maze test (***H***; $n = 11$). Data were expressed as mean ± SEM. For survival rate analysis, long-rank test was used. *$p < 0.05$ versus vehicle, for others one-way ANOVA with Bonferroni's *post hoc* test was used (*$p < 0.05$, **$p < 0.01$). WT, wild-type.

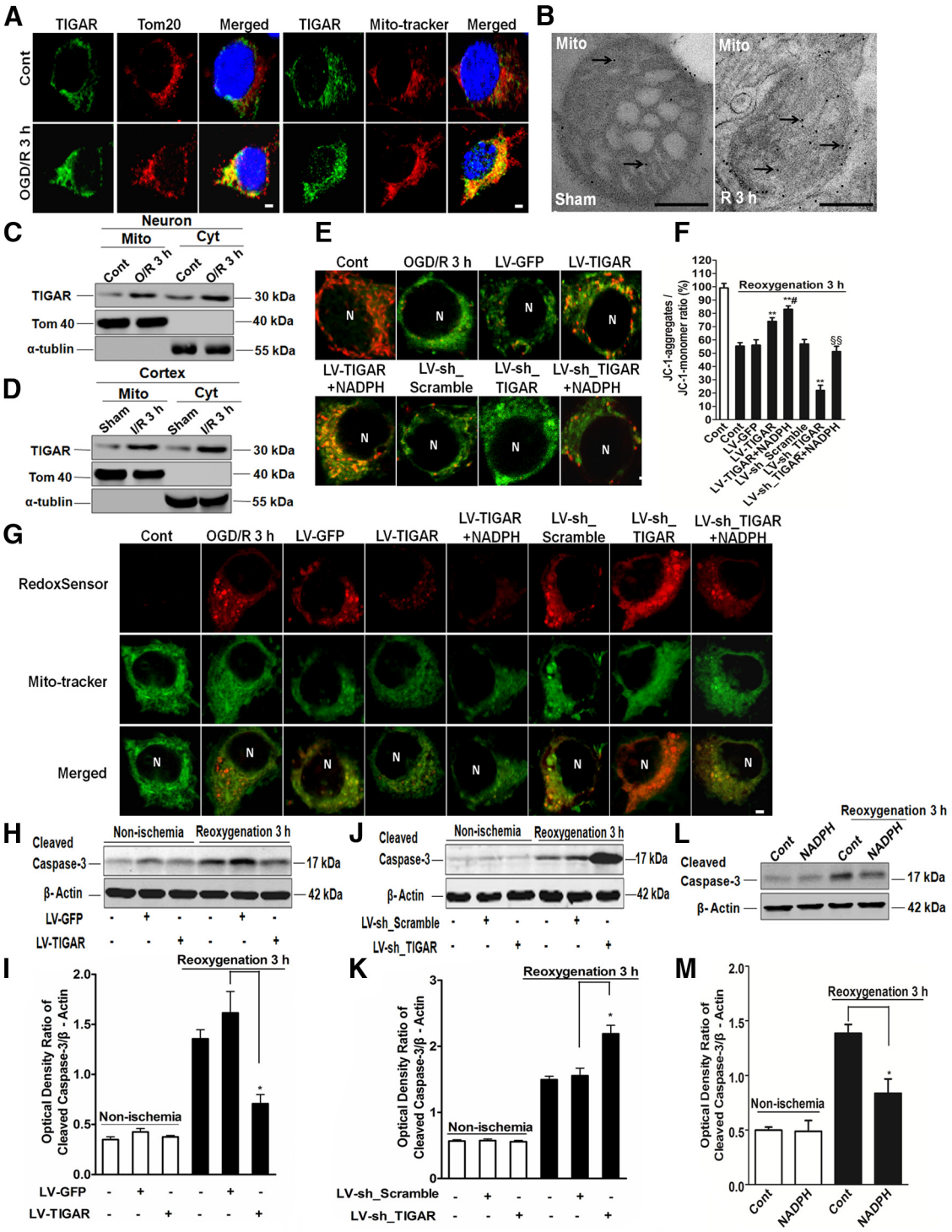

Figure 8. TIGAR mitochondrial translocation reduces mitochondria ROS, preserves mitochondria membrane potential, and inhibits caspase-3 activation. ***A***, Increased mitochondria localization of TIGAR 3 h after reoxygenation in cultured primary neurons; $n = 5$. Scale bar, 10 μm. Cont, control. ***B***, TIGAR mitochondrial translocation in mice brain cortical tissues after reperfusion (Mito; indicated by arrows). Scale bar, 200 nm. ***C***, The expression of TIGAR protein in the mitochondria was increased in primary cortical neurons after reoxygenation. Cyt, cytoplasm. ***D***, The expression of TIGAR protein in the mitochondria in mice brain cortex tissues was increased after reperfusion. ***E***, ***F***, Changes in mitochondria membrane potential. Representative fluorescence image of JC-1 staining (10 μM) and flow cytometer analysis of orange and green fluorescence signal of JC-1. Existence of JC-1 in healthy mitochondria was shown by aggregates emitting orange fluorescent after being inspired, but it distributed as diffused monomers emitting green fluorescence in depolarized mitochondria suffered from OGD/reoxygenation ($^{**}p < 0.01$ vs cont, $^{\#}p < 0.05$ vs LV-TIGAR, $^{\S\S}p < 0.01$ vs LV-sh_TIGAR under reoxygenation condition; $n = 5$). Scale bar, 10 μm. ***G***, TIGAR deceased mitochondria ROS. N, nucleus. Scale bar, 10 μm. Duplicates of three independent experiments were analyzed for each group. ***H–K***, Immunoblots analysis of activated caspase-3 ($^{*}p < 0.05$, $n = 5$). Lentivirus-mediated TIGAR overexpression decreased caspase-3 activation, while knockdown of TIGAR increased caspase-3 activation ($^{*}p < 0.05$, $n = 5$). ***L***, ***M***, The exogenous NADPH inhibited the activation of caspase-3 under reoxygenation condition ($^{*}p < 0.05$, $n = 3$). Data were expressed as mean ± SEM. One-way ANOVA with Bonferroni's *post hoc* test.

genation or ischemia/reperfusion increased mitochondria localization of TIGAR. TIGAR overexpression reduced mitochondrial ROS, preserved mitochondrial membrane potential, reduced caspase-3 activation, and increased neuronal survival, while knockdown of TIGAR produced opposite effects. Furthermore, the neuroprotective effects of TIGAR upregulation were mimicked by supplementation with exogenous NADPH. Therefore, TIGAR protects neurons against ischemia/reperfusion-induced injury, at least partly, by increasing supply of NADPH and preserving mitochondria function.

It is well known that neurons have a lower glycolytic rate than astrocytes (Almeida et al., 2001) due to low PFKFB3 activity (Almeida et al., 2004). TIGAR shares partial structural similarity with the PFKFB family and functions as fructose-2,6-bisphosphatase (Bensaad et al., 2006; Li and Jogl, 2009; Mor et al., 2011), reducing glycolytic rate and promoting the PPP (a metabolic route involved in the generation of NADPH/GSH; Almeida et al., 2004). We found that TIGAR levels were robustly elevated in the mouse brains after ischemic/reperfusion treatment and in primary neurons after OGD/reoxygenation. It has been reported that TIGAR is a TP53-responsive gene, and its expression sometimes is TP53 independent, as shown by the data that TP53-null cells showed high basal levels of TIGAR protein expression (Bensaad et al., 2006). Our recent studies in cancer cells also found that TIGAR induction in response to doxorubicin treatment involved both TP53-dependent and -independent mechanisms (our unpublished observation). In this study, we found that induction of TIGAR was earlier than that of TP53 and TP53 inhibitor PFT-α, and that TP53 knockdown did not block the elevation of TIGAR, showing that additional mechanisms other than TP53 are involved in upregulation of TIGAR in the neurons under ischemia/reperfusion condition. These results suggest that multiple mechanisms may exist in regulation of TIGAR expression in different types of cells. Our unpublished observations suggest that the serum glucose, some hormones (e.g., adrenaline and glucocorticoid) that influence blood glucose, and ROS were implicated in the upregulation of TIGAR expression.

ROS play a major pathogenic role in ischemia/reperfusion brain injury. ROS are generated primarily from the mitochondria (Niizuma et al., 2009) and NOX-mediated reaction (Bedard and Krause, 2007; Kleinschnitz et al., 2010). ROS cause oxidative damage of proteins, lipids, and organelles inside of cells. Inhibiting the production of or removing ROS shows neuroprotection in a variety of ischemia/reperfusion models (Crack and Taylor, 2005; Webster et al., 2006). In the present study, upregulation of TIGAR and G6PD was expected to inhibit glycolytic activity and consequently promote the flux of PPP. The increased flow of the PPP enhanced the generation of NADPH, leading to increase of reduced GSH levels. Consistent with the notion, we found that neurons overexpressing TIGAR had higher NADPH and GSH levels and a concomitantly enhanced ability to scavenge the intracellular ROS, and thus attenuate oxidative stress. In loss-of-function approaches, we also showed that knockdown of TIGAR aggravated the oxidative injury in both *in vivo* and *in vitro* cerebral ischemia/reperfusion models due to lowered NADPH and GSH levels and increased levels of ROS. Furthermore, supplementing exogenous NADPH produced similar effects of TIGAR overexpression. We thus conclude that TIGAR is essential in ischemia/reperfusion injury by controlling intracellular ROS via NADPH. Although there is no dispute that oxidative stress is an important pathogenic mechanism of neuronal injury in ischemia/reperfusion condition, clinical application of antioxidants did not yield encouraging outcomes (Dirnagl et al., 1999). The lack of efficacy of antioxidants may be due to inability of these molecules to sufficiently reduce intracellular ROS, where most of the damage caused by ROS takes place. Thus TIGAR-regulated PPP metabolic pathway may be a more effective mechanism to combat oxidative stress.

NOXs are a family of enzymes that generate superoxide by transferring electrons from NADPH to molecular oxygen via flavins within their structure. NOX-related oxidative stress could cause neuronal damage in ischemic stroke (Kleinschnitz et al., 2010). In this study, we found that induction of TIGAR was earlier than that of NOX4 and application of NADPH could increase GSH content rather than cause elevation of ROS levels. These results suggest that an increase in endogenous NADPH caused by upregulation of TIGAR would not generate more ROS through NOX4 under ischemia/reperfusion condition.

It is reported that TIGAR was also localized to mitochondria and interacted with hexokinase 2 to regulate mitochondrial membrane potential and mitochondrial ROS (Cheung et al., 2012). We confirmed the mitochondrial localization of TIGAR with immunogold and also observed an increase in mitochondrial localization of TIGAR under ischemia/reperfusion and OGD/reoxygenation conditions, thus we thought that TIGAR could protect mitochondria functions. Our findings showed that knockdown of TIGAR further decreased the mitochondrial membrane potential, increased mitochondrial ROS, increased caspase-3 activation, and triggered mitochondria-mediated apoptosis of injured neurons. TIGAR knockdown-induced exacerbation of OGD-induced mitochondrial changes, activation of caspase-3, and neuronal death were reversed by administration of exogenous NADPH. In contrast, overexpression of TIGAR produced beneficial effects to mitochondria. Therefore, TIGAR protects neurons against ischemia/reperfusion-induced injury by its ability to remove intracellular ROS and preservation of mitochondria functions.

We speculate that increased production of NADPH through PPP may also be beneficial for energy supply in neurons (Urner and Sakkas, 2005; Stanton, 2012). In particular, when there is a surplus supply of exogenous NADPH, some NADPH may be used for ATP production. It is also possible that increased supply of ribose may be required for rapid repair of DNA damage caused by oxidative stress during ischemia/reperfusion, as our preliminary studies showed that knockdown of TIGAR delayed the repair of anti-cancer drug-induced DNA breaks (our unpublished observations). These other mechanisms are possibly involved in neuroprotection by PPP and will be studied in the future.

Contrary to our observations, there was a report that cardiac damage induced by hypoxia (Kimata et al., 2010) or ischemia (Hoshino et al., 2012) was attenuated by knock out of TIGAR due to enhanced mitophagy, although TIGAR downregulation elevated ROS production. Many other reports have shown that the effects of TIGAR expression on cell survival are likely to be cell and context dependent. In several cancer cell lines, overexpression of TIGAR protected from ROS or TP53 induced apoptotic responses, but enhanced apoptosis in the IL-3-deprived lymphocytic cell line (Bensaad et al., 2006). Therefore, we suggest that different cellular metabolic background may determine a role of TIGAR in cell survival, and in the brain, for example, TIGAR upregulation clearly demonstrates a robust neuroprotection.

In summary, current studies demonstrated, for the first time, that upregulation of TIGAR protected neurons against ischemic

brain damage. TIGAR promoted neuronal survival through increasing flux of PPP and protection of mitochondrial functions. Our data thus elucidate a TIGAR-regulated metabolic pathway that offers strong neuroprotection against ischemic brain injury and suggest it may be a new therapeutic target for stroke prevention and treatment.

References

Almeida A, Almeida J, Bolaños JP, Moncada S (2001) Different responses of astrocytes and neurons to nitric oxide: the role of glycolytically generated ATP in astrocyte protection. Proc Natl Acad Sci U S A 98:15294–15299. CrossRef Medline

Almeida A, Moncada S, Bolaños JP (2004) Nitric oxide switches on glycolysis through the AMP protein kinase and 6-phosphofructo-2-kinase pathway. Nat Cell Biol 6:45–51. CrossRef Medline

Balaban RS, Nemoto S, Finkel T (2005) Mitochondria, oxidants, and aging. Cell 120:483–495. CrossRef Medline

Bedard K, Krause KH (2007) The NOX family of ROS-generating NADPH oxidases: physiology and pathophysiology. Physiol Rev 87:245–313. CrossRef Medline

Bensaad K, Tsuruta A, Selak MA, Vidal MN, Nakano K, Bartrons R, Gottlieb E, Vousden KH (2006) TIGAR, a p53-inducible regulator of glycolysis and apoptosis. Cell 126:107–120. CrossRef Medline

Chen H, Yoshioka H, Kim GS, Jung JE, Okami N, Sakata H, Maier CM, Narasimhan P, Goeders CE, Chan PH (2011) Oxidative stress in ischemic brain damage: mechanisms of cell death and potential molecular targets for neuroprotection. Antioxid Redox Signal 14:1505–1517. CrossRef Medline

Chen J, Li Y, Wang L, Zhang Z, Lu D, Lu M, Chopp M (2001) Therapeutic benefit of intravenous administration of bone marrow stromal cells after cerebral ischemia in rats. Stroke 32:1005–1011. CrossRef Medline

Cheung EC, Ludwig RL, Vousden KH (2012) Mitochondrial localization of TIGAR under hypoxia stimulates HK2 and lowers ROS and cell death. Proc Natl Acad Sci U S A 109:20491–20496. CrossRef Medline

Clark WM, Lessov NS, Dixon MP, Eckenstein F (1997) Monofilament intraluminal middle cerebral artery occlusion in the mouse. Neurol Res 19:641–648. Medline

Crack PJ, Taylor JM (2005) Reactive oxygen species and the modulation of stroke. Free Radic Biol Med 38:1433–1444. CrossRef Medline

Dirnagl U, Iadecola C, Moskowitz MA (1999) Pathobiology of ischaemic stroke: an integrated view. Trends Neurosci 22:391–397. CrossRef Medline

Hamm RJ, Pike BR, O'Dell DM, Lyeth BG, Jenkins LW (1994) The rotarod test: an evaluation of its effectiveness in assessing motor deficits following traumatic brain injury. J Neurotrauma 11: 187–96. CrossRef Medline

Herrero-Mendez A, Almeida A, Fernández E, Maestre C, Moncada S, Bolaños JP (2009) The bioenergetic and antioxidant status of neurons is controlled by continuous degradation of a key glycolytic enzyme by APC/C-Cdh1. Nat Cell Biol 11:747–752. CrossRef Medline

Hoshino A, Matoba S, Iwai-Kanai E, Nakamura H, Kimata M, Nakaoka M, Katamura M, Okawa Y, Ariyoshi M, Mita Y, Ikeda K, Ueyama T, Okigaki M, Matsubara H (2012) p53-TIGAR axis attenuates mitophagy to exacerbate cardiac damage after ischemia. J Mol Cell Cardiol 52:175–184. CrossRef Medline

Jain M, Cui L, Brenner DA, Wang B, Handy DE, Leopold JA, Loscalzo J, Apstein CS, Liao R (2004) Increased myocardial dysfunction after ischemia-reperfusion in mice lacking glucose-6-phosphate dehydrogenase. Circulation 109:898–903. CrossRef Medline

Kimata M, Matoba S, Iwai-Kanai E, Nakamura H, Hoshino A, Nakaoka M, Katamura M, Okawa Y, Mita Y, Okigaki M, Ikeda K, Tatsumi T, Matsubara H (2010) p53 and TIGAR regulate cardiac myocyte energy homeostasis under hypoxic stress. Am J Physiol Heart Circ Physiol 299: H1908–16. CrossRef Medline

Kleinschnitz C, Grund H, Wingler K, Armitage ME, Jones E, Mittal M, Barit D, Schwarz T, Geis C, Kraft P, Barthel K, Schuhmann MK, Herrmann AM, Meuth SG, Stoll G, Meurer S, Schrewe A, Becker L, Gailus-Durner V, Fuchs H, et al. (2010) Post-stroke inhibition of induced NADPH oxidase type 4 prevents oxidative stress and neurodegeneration. PLoS Biol 8:e1000479. CrossRef Medline

Kuwajima M, Hall RA, Aiba A, Smith Y (2004) Subcellular and subsynaptic localization of group I metabotropic glutamate receptors in the monkey subthalamic nucleus. J Comp Neurol 474:589–602. CrossRef Medline

Leker RR, Aharonowiz M, Greig NH, Ovadia H (2004) The role of p53-induced apoptosis in cerebral ischemia: effects of the p53 inhibitor pifithrin alpha. Exp Neurol 187:478–486. CrossRef Medline

Li H, Jogl G (2009) Structural and biochemical studies of TIGAR (TP53-induced glycolysis and apoptosis regulator). J Biol Chem 284:1748–1754. CrossRef Medline

Lin MT, Beal MF (2006) Mitochondrial dysfunction and oxidative stress in neurodegenerative diseases. Nature 443:787–795. CrossRef Medline

Longa EZ, Weinstein PR, Carlson S, Cummins R (1989) Reversible middle cerebral artery occlusion without craniectomy in rats. Stroke 20:84–91. CrossRef Medline

Mdzinarishvili A, Kiewert C, Kumar V, Hillert M, Klein J (2007) Bilobalide prevents ischemia-induced edema formation in vitro and in vivo. Neuroscience 144:217–222. CrossRef Medline

Mor I, Cheung EC, Vousden KH (2011) Control of glycolysis through regulation of PFK1: old friends and recent additions. Cold Spring Harb Symp Quant Biol 76:211–216. CrossRef Medline

Müller HD, Hanumanthiah KM, Diederich K, Schwab S, Schäbitz WR, Sommer C (2008) Brain-derived neurotrophic factor but not forced arm use improves long-term outcome after photothrombotic stroke and transiently upregulates binding densities of excitatory glutamate receptors in the rat brain. Stroke 39:1012–1021. CrossRef Medline

Niizuma K, Endo H, Chan PH (2009) Oxidative stress and mitochondrial dysfunction as determinants of ischemic neuronal death and survival. J Neurochem 109 [Suppl 1]:133–138. CrossRef Medline

Sims NR, Muyderman H (2010) Mitochondria, oxidative metabolism and cell death in stroke. Biochim Biophys Acta 1802:80–91. CrossRef Medline

Stanton RC (2012) Glucose-6-phosphate dehydrogenase, NADPH, and cell survival. IUBMB Life 64:362–369. CrossRef Medline

Tamatani M, Matsuyama T, Yamaguchi A, Mitsuda N, Tsukamoto Y, Taniguchi M, Che YH, Ozawa K, Hori O, Nishimura H, Yamashita A, Okabe M, Yanagi H, Stern DM, Ogawa S, Tohyama M (2001) ORP150 protects against hypoxia/ischemia-induced neuronal death. Nat Med 7:317–323. CrossRef Medline

Urner F, Sakkas D (2005) Involvement of the pentose phosphate pathway and redox regulation in fertilization in the mouse. Mol Reprod Dev 70: 494–503. CrossRef Medline

Webster KA, Graham RM, Thompson JW, Spiga MG, Frazier DP, Wilson A, Bishopric NH (2006) Redox stress and the contributions of BH3-only proteins to infarction. Antioxid Redox Signal 8:1667–1676. CrossRef Medline

Yamada K, Tanaka T, Zou LB, Senzaki K, Yano K, Osada T, Ana O, Ren X, Kameyama T, Nabeshima T (1999) Long-term deprivation of oestrogens by ovariectomy potentiates beta-amyloid-induced working memory deficits in rats. Br J Pharmacol 128:419–427. CrossRef Medline

Yin L, Kosugi M, Kufe D (2012) Inhibition of the MUC1-C oncoprotein induces multiple myeloma cell death by downregulating TIGAR expression and depleting NADPH. Blood 119:810–816. CrossRef Medline

Yonekura I, Takai K, Asai A, Kawahara N, Kirino T (2006) p53 potentiates hippocampal neuronal death caused by global ischemia. J Cereb Blood Flow Metab 26:1332–1340. CrossRef Medline

Zhang F, Wang S, Signore AP, Chen J (2007) Neuroprotective effects of leptin against ischemic injury induced by oxygen-glucose deprivation and transient cerebral ischemia. Stroke 38:2329–2336. CrossRef Medline